Functional Analysis of the Cellulose Synthase Genes *CesA1*, *CesA2*, and *CesA3* in Arabidopsis[1]

Joanne E. Burn, Charles H. Hocart, Rosemary J. Birch, Ann C. Cork, and Richard E. Williamson*

Plant Cell Biology Group, Research School of Biological Sciences, Australian National University, G.P.O. Box 475, Canberra, Australian Capital Territory 2601, Australia

Polysaccharide analyses of mutants link several of the glycosyltransferases encoded by the 10 *CesA* genes of Arabidopsis to cellulose synthesis. Features of those mutant phenotypes point to particular genes depositing cellulose predominantly in either primary or secondary walls. We used transformation with antisense constructs to investigate the functions of *CesA2* (*AthA*) and *CesA3* (*AthB*), genes for which reduced synthesis mutants are not yet available. Plants expressing antisense *CesA1* (*RSW1*) provided a comparison with a gene whose mutant phenotype (Rsw1$^-$) points mainly to a primary wall role. The antisense phenotypes of *CesA1* and *CesA3* were closely similar and correlated with reduced expression of the target gene. Reductions in cell length rather than cell number underlay the shorter bolts and stamen filaments. Surprisingly, seedling roots were unaffected in both *CesA1* and *CesA3* antisense plants. In keeping with the mild phenotype compared with Rsw1$^-$, reductions in total cellulose levels in antisense *CesA1* and *CesA3* plants were at the borderline of significance. We conclude that *CesA3*, like *CesA1*, is required for deposition of primary wall cellulose. To test whether there were important functional differences between the two, we overexpressed *CesA3* in *rsw1* but were unable to complement that mutant's defect in *CesA1*. The function of CesA2 was less obvious, but, consistent with a role in primary wall deposition, the rate of stem elongation was reduced in antisense plants growing rapidly at 31°C.

Cellulose is the most abundant plant polysaccharide, providing mechanical support to individual cells and the whole plant. Cellulose microfibrils are spooled around each cell and, with hemicellulose bridges between the microfibrils, form a network that serves as the main load-bearing element of the plant and regulates the direction of cell expansion. Cell walls are categorized according to whether they are deposited during cell growth (primary) or after it ceases (secondary). Cells with strongly aligned cellulose expand anisotropically, favoring expansion along the direction of least resistance (perpendicular to the microfibrils) and restricting growth in diameter (parallel to the microfibrils). This directional cell expansion is then translated into the direction of expansion of the entire organ.

Cellulose is synthesized by structures in the plasma membrane known as rosettes (Brown et al., 1996). There are fewer rosettes in mutants that make less cellulose such as the Arabidopsis *rsw1-1* mutant (Arioli et al., 1998) and the barley (*Hordeum vulgare*) brittle culm mutant (Kimura et al., 1999b). Recent progress has identified genes encoding two classes of enzymes important in cellulose synthesis: members of a family of *CesA* glycosyltransferases (for review, see Richmond, 2000) and one member of a small family of membrane-bound endo-1,4-β-glucanases (Nicol et al., 1998; Zuo et al., 2000; Lane et al., 2001; Sato et al., 2001).

Pear et al. (1996) identified a gene encoding a putative glycosyltransferase that was strongly expressed during cellulose deposition in the developing cotton fiber. The protein showed weak homology to bacterial glycosyltransferases involved in cellulose synthesis, bound UDP-Glc, and was subsequently localized to the plasma membrane rosettes (Kimura et al., 1999a). Arabidopsis has a family of a least 10 such glycosyltransferases (Richard, 2000). They contain the conserved D,D,D,QXXRW motif characteristic of processive β-glycosyltransferases (Saxena et al., 1995), eight membrane spanning regions, and a putative zinc-binding domain that may be involved in protein-protein interaction.

Mutants link five of these genes to cellulose synthesis, and the mutant phenotypes point to each gene having a role predominantly in either primary or in secondary wall deposition. *CesA1* is mutated in the cellulose-deficient, radial swelling mutant *rsw1-1* (Arioli et al., 1998). Changing Ala-549 to Val gives a strong temperature-sensitive phenotype. *rsw1-1* grown at the restrictive temperature is severely stunted and has smaller cells that often bulge out from the organ surface. Plants grown continuously at the restrictive temperature form a few tiny leaves with only a small minority producing bolts carrying severely malformed flowers (Williamson et al., 2001). The extensive morphological alterations indicate that CesA1 synthesizes cellulose for primary cell walls, and this is directly demonstrated by changed wall

[1] This work was supported in part by a grant from North Eucalypt Technologies (to J.E.B.).

* Corresponding author; e-mail richard@rsbs.anu.edu.au; fax 61–2–6125–4331.

Article, publication date, and citation information can be found at www.plantphysiol.org/cgi/doi/10.1104/pp.010931.

ultrastructure in mitotic and expanding root cells (Sugimoto et al., 2001). Mutations in *CesA6* (*PROCUSTE*; Fagard et al., 2000) result in a similar phenotype, again consistent with deposition of primary cell wall cellulose. While this manuscript was in preparation, Scheible et al. (2001) demonstrated that mutations in *CesA3* (and *CesA6*) confer resistance to isoxaben, a herbicide specifically inhibiting cellulose. Because isoxaben causes radial swelling of roots, this indicates that CesA3 probably also contributes cellulose to primary walls. In contrast, the *irx1* and *irx3* mutants (mutated in the *CesA8* and *CesA7* genes, respectively; Taylor et al., 1999, 2000) do not show major changes in organ size and shape but show collapsed xylem elements attributable to reduced cellulose deposition in secondary cell walls (Turner and Somerville, 1997). *CesA4* has also been suggested to be involved in cellulose synthesis for secondary cell walls on the basis of β-glucuronidase expression driven by the *CesA4* promoter (Holland et al., 2000).

The evidence, therefore, favors roles in primary cell wall deposition for *CesA1*, *CesA3*, and *CesA6* and roles in secondary cell wall deposition for *CesA7* and *CesA8*. The strong phenotypes seen when *CesA1*, *6*, *7*, and *8* are mutated show that the genes are nonredundant, but this does not necessarily mean that they perform unique functions. The latter case has been argued (Fagard et al., 2000; Taylor et al., 2000; Scheible et al., 2001), but mutant phenotypes alone cannot establish whether proteins serve unique functions even when a mutation is lethal. For example, yeast has two α-tubulin genes, TUB1 and TUB3 (Schatz et al., 1986). Null alleles of TUB1 are lethal, whereas null alleles of TUB3 produce less severe phenotypes. Neither serves unique functions that cannot be undertaken by the other, however, because Schatz et al. found that TUB1 or TUB3 complemented mutations in the other gene if strongly expressed. The question of whether individual *CesA* genes perform functions that other genes cannot should, therefore, remain open even in cases (such as *CesA1*) where mutations are conditionally lethal.

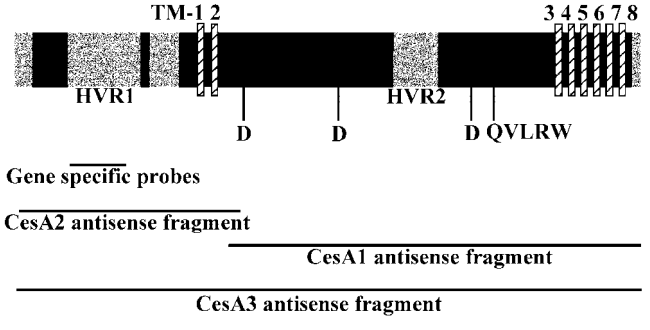

Figure 1. Locations of gene-specific probes and antisense fragments within the conserved structure of *CesA* proteins. All *CesA* proteins have eight transmembrane (TM) domains (hatched) and the amino acid motif D,D,D,QVLRW. Regions shown in black have conserved amino acid sequence, whereas the gray regions do not (HVR, hypervariable region). Gene-specific probes were designed to the HVR1 of each gene. The length and position of the DNA fragment used in each of the antisense constructs is also shown.

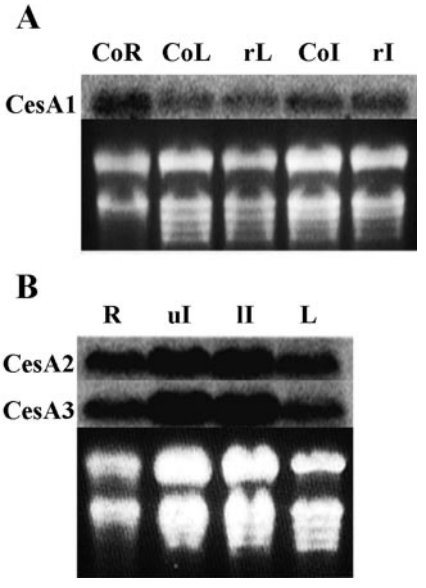

Figure 2. Expression patterns of *CesA1*, *CesA2*, and *CesA3*. Total RNA was isolated from roots (R), inflorescence (I), and rosette leaves (L) of Columbia (Co) grown at 21°C and of *rsw1-1* (r) grown at 31°C. In some cases, the inflorescence material was split into upper inflorescence (uI) containing stem, meristem, buds, flowers, and cauline leaves and a lower inflorescence (lI) containing only cauline leaves and lower stem, respectively. Blots were probed with gene-specific riboprobes of *CesA1* (A), *CesA2*, and *CesA3* (B). The RNA loading is seen in the ethidium bromide-stained gels shown below. All genes are strongly expressed in all tissues, and there are no major changes in the level of *CesA1* mRNA in *rsw1-1*.

In this study, we used antisense technology to explore the previously unknown functions of the *CesA2* gene. We also used antisense technology to establish the relative importance of *CesA1* and *CesA3* for cellulose synthesis in all growing organs, and we overexpressed *CesA3* in the *CesA1* mutant *rsw1-1* to provide a more rigorous genetic test of whether CesA1 and CesA3 perform functions that the other cannot replicate even when overexpressed.

RESULTS

Gene Expression

The sequences amplified from the hypervariable region of each gene (Fig. 1) hybridized only to the corresponding gene (data not shown). Total RNA probed with each gene-specific PCR product showed that transcripts of the predicted sizes for each gene were expressed at similar levels in leaf, inflorescence, and root (Fig. 2). Hybridization to RNA derived from leaf and inflorescence tissue of *rsw1-1* grown at its restrictive temperature showed that the mutant allele was expressed at a similar level to the wild-type allele and that the size of the transcript was identical

(consistent with the single nucleotide change detected in the mutant by Arioli et al., 1998).

Molecular Analysis of Antisense Plants

Wild-type Arabidopsis was transformed with 35S::antisense constructs of *CesA1*, *CesA2*, and *CesA3* (Fig. 1), and T_1 kanamycin-resistant transformants were selected. Readily visible differences in growth and morphology (described below) were found in 17 of 89 resistant T_1 plants transformed with the *CesA1* construct and in eight of 24 T_1 plants transformed with *CesA3* but in none of 267 plants transformed with *CesA2*. The *CesA1* and *CesA*3 phenotypes were, however, markedly unstable, and only eight of those 17 antisense *CesA1* lines and only three of the eight *CesA3* lines retained the phenotype in the T_3 generation. Even homozygous lines continued to segregate T_3 individuals with wild-type phenotype.

RNA from T_2 antisense plants was probed with gene-specific riboprobes. The data (Fig. 3) show that: (a) all *CesA2* antisense plants have reduced expression of the target gene even though they lack a readily visible phenotype; (b) *CesA1* and *CesA3* plants that have reverted to a wild-type phenotype (e.g. lane 3 for *CesA*1; lanes 3, 4, and 9 for *CesA*3) show near wild-type expression of the target gene; and (c) only expression of the target gene is reduced. The *CesA10* gene (chromosome 2) is particularly closely related to *CesA1* (chromosome 4) probably because of a chromosomal duplication event (http://mips.gsf.de/proj/thal/). *CesA10* is very weakly expressed in inflorescences (Fig. 3) but is still detectable in plants in which expression of *CesA1* has been severely reduced (lane 10 of Fig. 3).

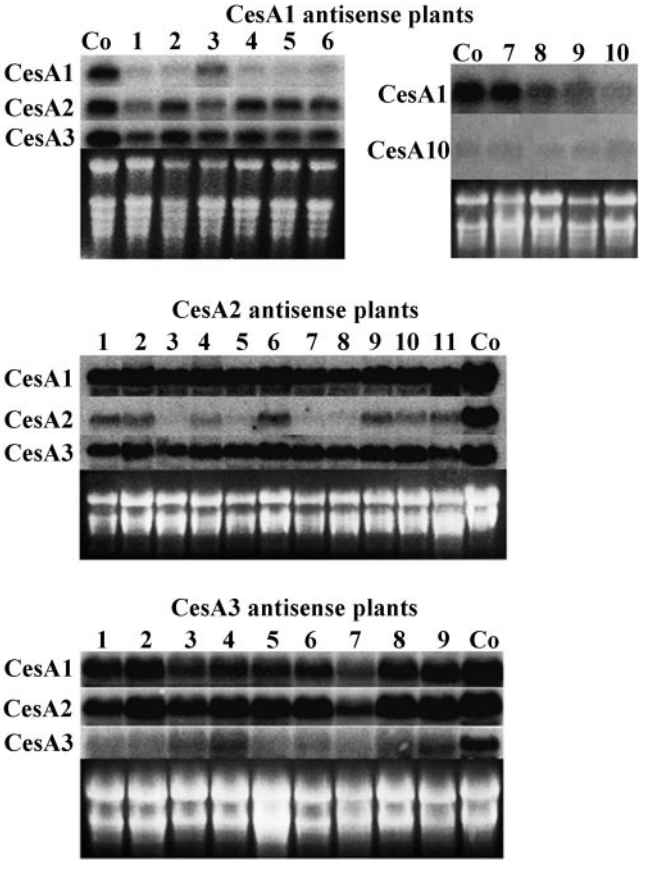

Figure 3. CesA gene expression in antisense plants. Total RNA from rosette leaves of T_2 plants carrying antisense constructs of *CesA1*, *CesA2*, and *CesA3* and from Columbia (Co) was resolved by agarose gel electrophoresis and probed with specific *CesA1*, *CesA2*, and *CesA3* probes, and the gel was stained with ethidium bromide to show the loading. A probe to the *CesA10* gene was also used to probe RNA from the inflorescences of some *CesA1* antisense plants (lanes 7–10) and a Co control because *CesA1* and *CesA10* are particularly closely related. The results show (a) that only expression of the targeted *CesA* gene was reduced even in the case of *CesA10* in *CesA1* antisense plants; (b) that plants that have reverted to a wild-type phenotype (lane 3 for *CesA1* antisense; lanes 3, 4, and 9 for *CesA3* antisense) show much higher expression of the target gene than plants that continue to show the antisense phenotype; and (c) that *CesA2* expression was successfully reduced by its antisense construct, even though only a minimal phenotype was observed.

Morphology of *CesA1* and *CesA3* Antisense Plants

Plants from the 12 *CesA1* and six *CesA*3 lines that retained an altered T_2 phenotype were compared with wild type and with the *rsw1-1* mutant grown at its restrictive temperature. The phenotypes of plants containing *CesA1* and *CesA3* constructs were closely similar to each other and showed increasing severity during development.

Surprisingly, all tested *CesA1* and *CesA3* antisense lines showed normal seedling root growth quite unlike the *rsw1-1* mutant whose root swells and extends much more slowly at the restrictive temperature (Baskin et al., 1992). Hypocotyls and cotyledons, likewise, appeared normal. The blades and particularly the petioles of rosette leaves were, however, much smaller in the severe antisense lines (Fig. 4A), although propagation to the T_3 generation reduced the severity of the effect (Fig. 4B). Pavement cells had less complex shapes than in wild type, appeared slightly swollen, and in some regions of the leaf, groups of cells bulged outwards (Fig. 4, C–E). Trichomes appeared normal in all antisense lines, although the cells at the base of the trichome were swollen (Fig. 4, F and G). Both *CesA1* and *CesA3* antisense lines showed wild-type patterns of leaf initiation with 14- and 21-d-old plants having identical numbers of leaves in wild-type and antisense plants.

All T_2 antisense lines and wild type initiated reproductive growth at about 21 d, but *CesA1* and *CesA3* antisense bolts were much shorter (Fig. 6A) and thinner (not shown). The internal structure of the bolt seen in cross-section appeared unaltered, and xylem vessels showed spiral thickenings with similar thickness to wild type when viewed by cryoscanning electron microscopy. All antisense lines produced many more side branches, and the primary stem often

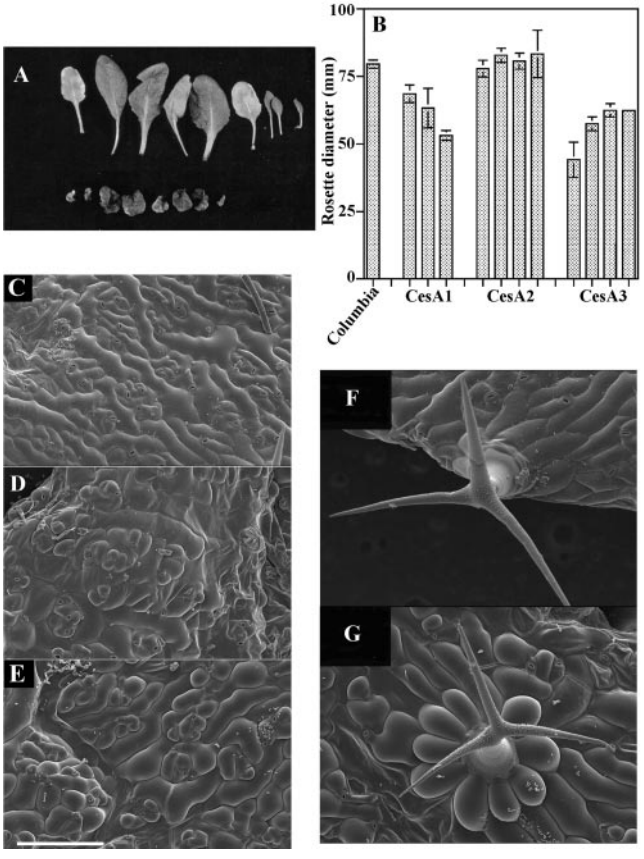

Figure 4. Morphology of rosette leaves. A, Rosette leaves, and in particular petioles, from a 28-d-old wild-type plant (top row) are much bigger than those from a T_2 *CesA3* antisense plant. B, Rosette diameter of T_3 lines, measured on d 35, show that *CesA1* and *CesA3* lines but not *CesA2* lines are smaller than wild type (means of $n \geq 2$; bars show SE). The plants measured to provide the first column of the *CesA3* plants are descended from the T_2 plant shown in A. The reduced severity of the T_3 phenotype is apparent. C through E, Cryoscanning electron micrographs showing that the complex shapes of pavement cells in wild-type plants (C) are much simpler in antisense plants carrying *CesA1* (D) and *CesA3* (E) constructs. F and G, Cryoscanning electron micrographs of trichomes in wild-type (F) and *CesA3* antisense (G) plants. Cells at the base of the trichome are greatly swollen in antisense plants. Bar = 200 μm.

failed to develop further after initiating a few flowers with a side shoot frequently becoming the tallest stem. Cauline leaves appeared normal; pavement cells maintained their complex shapes and normal trichomes and stomata developed. All *CesA1* and *CesA3* antisense lines showed greatly reduced fertility, with the severest lines producing no seed. Flower parts were smaller than wild type (Figs. 5, A–C, and 6B), although the gynoecium was reduced less severely than other parts so that the stigma protruded well beyond the petals, which, in turn, did not protrude from beneath the sepals. Cells on the sepals were often swollen, particularly in *CesA3* antisense lines (Fig. 5, D and E), but trichomes and stomata developed normally. The anthers released pollen of wild-type appearance but it was not deposited onto the papillae because the stamen filaments were very short (Figs. 5, A–C, and 6B). Seed set was still reduced relative to wild type when antisense lines were manually self-pollinated, showing that physical separation was not the only problem for self-fertilization. The reduction in seed number correlated with the intensity of the visible phenotype, with plants showing the severest phenotype setting no seed even after hand pollination (data not shown). Reciprocal crosses with wild type showed that the female reproductive capacity was more strongly affected in the antisense plants than was male capacity.

Effects on Cell Elongation and Division

We used stamen filaments and stems to determine whether reductions in cell expansion or cell division reduced organ lengths in *CesA1* and *CesA3* antisense plants. Reductions in cell length (Fig. 6C) rather than cell number (Fig. 6D) account for almost all of the reduction in stamen filament lengths in both antisense and *rsw1-1* plants. Because such a method determines only final cell number, slower cell production could be masked if the period over which cell division occurred was extended. Therefore, when we looked at the stem, we used a simple kinematic method to compare wild-type and antisense plants for cell flux, the number of cells that exited the stem's elongation zone in a 24-h period (Silk et al., 1989).

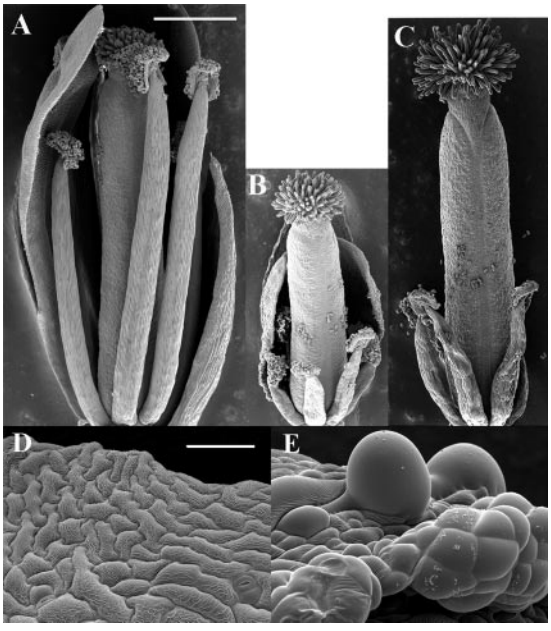

Figure 5. Cryoscanning electron micrographs showing flower morphology. A through C, General morphology seen after removing some sepals and petals from wild-type (A), *CesA1* (B), and *CesA3* (C) antisense plants. All floral organs are reduced in length in both antisense lines, but reductions in gynoecium length are less severe so that the stigma protrudes beyond the petals in the antisense plants. Bar = 500 μm. D and E, Swelling of sepal cells is seen in *CesA3* antisense plants (E) but not wild-type plants (D). Bar = 50 μm.

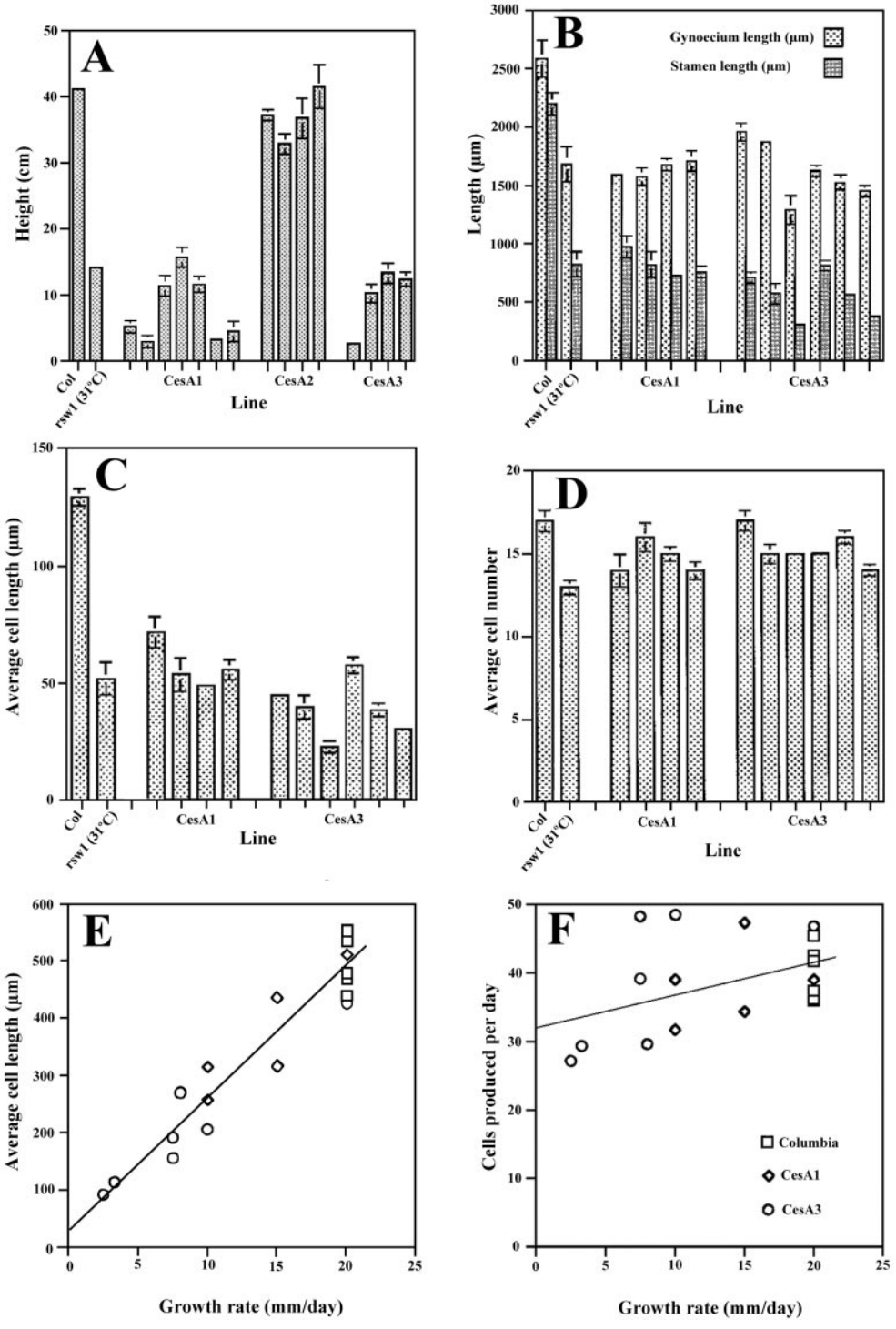

Figure 6. Reduced cell expansion rather than reduced cell production contributes most to organ size reduction. A, Final stem lengths (mean ± SE, $n \geq 10$) of wild-type and T_2 antisense plants (all grown at 21°C) and of *rsw1-1* plants grown at 21°C just until initiated bolts were removed, and the plants were transferred to 31°C to follow stem regrowth. *CesA1* and *CesA3* antisense reduces height much more than *CesA2* does, although the second and third columns of *CesA2* results are significantly different from wild type. B, Lengths (mean ± SE, $n \geq 5$) of the gynoecium and stamen filaments in *CesA1* and *CesA3* antisense plants, in *rsw1-1* grown as above, and in wild-type Columbia plants. Antisense and *rsw1-1* reduce stamen filament lengths more severely than gynoecium length. Lengths measured by cryoscanning electron microscopy. C and D, Large reductions in cell length (C) but only small reductions in cell number (D) in cell files from stamen filaments (mean ± SE, $n \geq 5$). E and F, Kinematic analysis of stem elongation in wild-type and *CesA1* and *CesA3* antisense plants. Growth rate correlates strongly with cell length (E) but only weakly with cell flux (F), the number of cells exiting the elongation zone per day. Lines fitted by linear regression with $r = 0.96$ in E and 0.46 in F.

There is a much stronger correlation between stem growth rate and cell length ($r = 0.96$) in the different lines of antisense plants (Fig. 6E) than between growth rate and cell flux ($r = 0.46$; Fig. 6F). In contrast, stems of the cellulose-deficient *rsw2-1* (mutated in gene encoding the KORRIGAN endocellulase) show only a 24% reduction in cell length but a 60% reduction in cell flux when grown at their restrictive temperature (Columbia wild type: growth rate = 38.8 ± 1.5 mm d^{-1}, cell length = 342.7 ± 8.6 μm, cell flux 113.8 ± 3.4; *rsw2-1*: growth rate = 11.4 ± 1.8 mm d^{-1}, cell length = 260.7 ± 9.5 μm, cell flux 45.1 ± 4.1; mean ± SE for 10 cells in each of six plants per line).

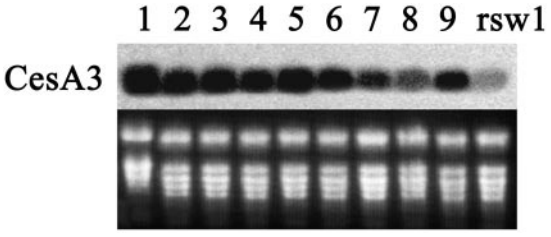

Figure 7. Overexpression of *CesA3* in *rsw1-1* plants transformed with the 35S::CesA3 construct. RNA from leaves of T2 plants and of the untransformed *rsw1-1* was probed with the gene-specific *CesA3* riboprobe. *CesA3* is overexpressed in all nine lines examined. RNA loading is shown in the lower panel.

Cellulose Content of Antisense Plants

The results presented so far are consistent with *CesA1* and *CesA3* antisense plants having a morphological phenotype that is broadly similar to but generally weaker than that of *rsw1-1* grown at 31°C. We, therefore, expected that antisense plants would show a smaller reduction in cellulose content than that found in *rsw1-1*. We compared the cellulose content of wild-type rosette leaves with the cellulose content of leaves from two T_2 lines of *CesA1* and two T_2 lines of *CesA3* antisense plants. Levels in all four antisense lines were less than those of wild type, but only the lowest of the *CesA3* lines reached significance at the 5% level in the Student's *t* test (33.09 ± 0.91 nmol Glc mg^{-1} tissue dry weight for wild type; 28.35 ± 1.56 and 30.09 ± 2.72 for two *CesA1* lines; 29.01 ± 2.37 and 25.57 ± 1.82 for two *CesA3* lines; mean ± SE for $n = 4$).

CesA3 Overexpression Cannot Complement *rsw1-1*

To test whether overexpression of *CesA3* could complement the *CesA1* deficiency in *rsw1-1* in the way seen with yeast α-tubulins (Schatz et al., 1986), *rsw1-1* was transformed with *CesA1* or *CesA3* cDNAs in the sense orientation behind the 35S promoter. Ninety of 95 kanamycin-resistant T_1 transformants expressing 35S::*CesA1* showed wild-type root growth at the restrictive temperature, demonstrating that *CesA1*, when driven by the 35S promoter, efficiently complements *rsw1-1*. In contrast, none of 160 kanamycin-resistant lines carrying *CesA3* showed wild-type root growth at 31°C. The results were similar when transformed plants were grown at 21°C until bolts had initiated, the bolts were chopped off at the base, and the plants were transferred to 31°C to regrow bolts at the restrictive temperature (Williamson et al., 2001). All 35S::*CesA1* transformants showing wild-type root growth produced tall, wild-type inflorescences, whereas all 35S::*CesA3* transformants showed a much shorter inflorescence. Even though *CesA3* could not complement the *rsw1-1* phenotype, it was successfully overexpressed in all nine *CesA3* transformants tested with northern blots (Fig. 7). The 35S promoter expresses green fluorescent protein (GFP) in all cells of the meristem and elongation zone (Ridge et al., 1999), and the successful complementation by the *CesA1* cDNA indicates that the promoter achieves a functionally adequate level of transgene expression.

Analysis of *CesA2* Antisense Plants

None of the T1 *CesA2* antisense transformants showed phenotypes visible by eye, but some T_2 lines grown at 21°C showed reductions in stem length that were small but statistically significant (5% level, Student's *t* test; Fig. 6A). To make it more likely that reduced *CesA2* expression would become limiting for growth, we grew plants at 31°C where wild type elongates more rapidly and reaches a greater final height. The antisense lines were derived from those showing the most severe reductions in *CesA2* expression (lanes 3, 5, 7, and 8 in the *CesA2* panel of Fig. 3). Under these conditions of accelerated growth, there was a significant reduction in the rate of elongation in plants from all four antisense lines tested, although the final heights were not significantly different (Fig. 8).

Because a CesA2 promoter-GFP construct expresses only in vascular tissue in mature regions as well as in dividing and expanding cells (J.E. Burn, unpublished data), we examined the 31°C-grown *CesA2* antisense plants by cryoscanning electron microscopy to see whether secondary wall thickness was reduced. There was no significant reduction (5% level, Student *t* test) in the average wall thickness of freeze-fractured xylem vessel elements in stems grown at 31°C (1,021 ± 41 nm for wild type transformed with the empty pBIN19 vector; 1,046 ± 40 nm, 1,022 ± 40 nm, 1,034 ± 39 nm, and 989 ± 42 nm for four independent lines of antisense plants; mean ± SE for $n \geq 25$).

DISCUSSION

The *CesA1*, *CesA2*, and *CesA3* genes are widely expressed in Arabidopsis, and antisense suppression of *CesA1* and *CesA3* produces strong, albeit unstable, phenotypes, whereas *CesA2* mRNA can be reduced

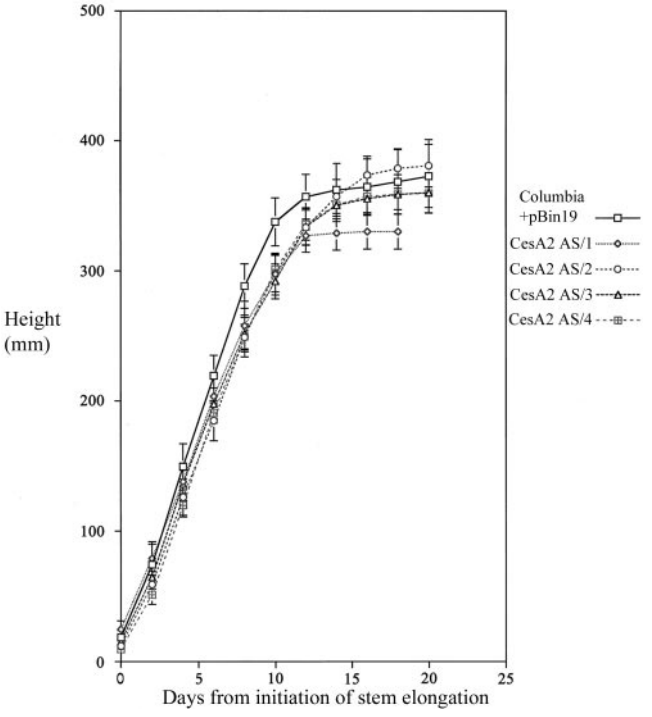

Figure 8. Growth in height of the stem of control and T2 antisense plants at 31°C. The heights of the stem were measured with a ruler at 2-d intervals and a mean height was calculated for at least five plants from the control and each of four antisense lines. Columbia wild-type transformed with the empty vector (Col + pBin19) was used as the control. The results show small but significant reductions in elongation rate in all four antisense lines.

and produce only a very mild phenotype. We will discuss what can be deduced regarding the function of these genes before looking in more general terms at the value of antisense approaches to assigning functions within the *CesA* gene family.

CesA1, *CesA3*, and *CesA6* in Primary Wall Deposition

Mutations in the *CesA1* (*rsw1* mutant; Arioli et al., 1998), *CesA6* (*prc*; Fagard et al., 2000), *CesA7* (*irx3*; Taylor et al., 1999), and *CesA8* (*irx1*; Taylor et al., 2000) genes reduce cellulose synthesis in Arabidopsis. As outlined in the introduction, the phenotypes fall into two classes pointing to the gene products being mainly required to deposit cellulose in primary walls (*CesA1* and *CesA6*) or in secondary walls (*CesA7* and *CesA8*). Changes to cell shape, growth, and morphogenesis result when changes to primary walls alter cell expansion and/or cell divisions. Changes to secondary walls occur too late to affect these processes so that morphology is normal but mechanical properties change.

Antisense phenotypes point to both CesA1 and CesA3 contributing to primary walls. The CesA1 information is confirmatory given that previous studies of *rsw1-1* showed morphological changes (Arioli et al., 1998; Williamson et al., 2001) and direct evidence of changes in primary wall ultrastructure (Sugimoto et al., 2001). The *CesA3* antisense phenotype and the overexpression experiment, however, give four functional insights that can be considered together with those arising from the study of Scheible et al. (2001), which focused on herbicide resistance.

First, we show that *CesA3* is of comparable importance to *CesA1* for growth. The *CesA3* antisense phenotype is essentially indistinguishable from the antisense phenotype of *CesA1.* The two antisense phenotypes and the *rsw1-1* phenotype show smaller leaves, shorter stems, smaller floral organs with stamen filament length reduced more than gynoecium length, reduced fertility even when manually pollinated, simplification of complex shapes of pavement cells on leaf surfaces, and bulging of some cells from organ surfaces. The antisense phenotype is dramatically weaker than the phenotype caused by continuously growing *rsw1-1* at 31°C, which produces minute plants that rarely initiate reproductive growth (Williamson et al., 2001). The difference is most dramatic in seedlings where there is no visible phenotype in antisense plants, although an obvious phenotype develops later during rosette development and reproductive growth. Some increase in the apparent severity of the antisense phenotype with progression through the life cycle might be expected for a constitutively expressed phenotype: Smaller rosette leaves could themselves restrict later stem elongation purely by supplying less photosynthate. The lack of phenotype in seedlings is, however, surprising and is discussed below.

Second, we show that *CesA3* and *CesA6* are not redundant for growth. Scheible et al. (2001) reasoned that *CesA3* and *CesA6* were redundant because mutations in either can confer isoxaben resistance but the effects of mutations in the two genes are not additive. There is no redundancy where growth is concerned, because the *CesA3* antisense construct dramatically reduced stem growth even though *CesA6* is expressed there (Fagard et al., 2000; J.E. Burn, unpublished data), and *procuste* (*CesA6* mutant) shows growth reductions (Fagard et al., 2000) in organs where we find *CesA3* expression.

Third, we show that *CesA3* cannot perform the functions of *CesA1* even when overexpressed under the control of a promoter that can complement *rsw1-1* when driving expression of a *CesA1* cDNA. This provides a much stronger genetic test of whether the two proteins have unique properties (see Schatz et al., 1986). Biochemical or other evidence of unique CesA function still remain desirable, however, before the issue of unique functions is regarded as settled.

Fourth, we show that down-regulation of *CesA3*, like down-regulation of *CesA1* and *CesA6*, strongly reduces cell expansion rather than division. The reduced size of stems and stamen filaments in *CesA1* and *CesA3* antisense plants and in *rsw1-1* all reflect much greater reductions in cell expansion than in cell

division rates, and a similar conclusion was reached for *CesA6* by kinematic analysis of root growth using *qui1* (Hauser et al., 1995), which was later shown to be allelic to *prc* and so mutated in *CesA6* (Fagard et al., 2000). Several *prc* alleles show incomplete walls in hypocotyl cells, but the complete walls in *prc* embryos suggests that the gaps arise during cell expansion rather than from defects in cytokinesis (Fagard et al., 2000). The evidence is, therefore, consistent with mutations in all three *CesA* genes having more profound effects on cell expansion than on cytokinesis. This provides an interesting contrast with the situation for *rsw2-1*, which is mutated in the KORRIGAN endocellulase and impaired in cellulose synthesis (Lane et al., 2001). *rsw2-1* shows clear reductions in cell number and cell size. Reductions in cell number may be attributable to targeting to the cell plate (Zuo et al., 2000). At the moment, there is no evidence that different CesA proteins are targeted to the cell plate or of *CesA* mutants that particularly affect the cell plate but differential intracellular targeting should not be neglected as a possible mechanism by which CesA proteins could be functionally differentiated.

Lack of Seedling Phenotype in *CesA1* and *CesA3* Antisense Plants

Growing *rsw1-1* at its restrictive temperature inhibits its root and hypocotyl elongation and promotes radial swelling (Baskin et al., 1992; Williamson et al., 2001), whereas neither *CesA1* nor *CesA3* antisense constructs cause any comparable changes. The differences could relate to differences between antisense suppression and properties specific to the *rsw1-1* allele or to more general features of antisense constructs. The *rsw1-1* mutant shows at least three subcellular changes that contribute in unknown proportions to the visible seedling phenotype: Seedlings have less cellulose (Arioli et al., 1998; Peng et al., 2000), more readily extractable glucan (Arioli et al., 1998), and impaired microfibril alignment (Sugimoto et al., 2001). One of these subcellular changes may be essential to development of the visible seedling phenotype and not produced by antisense. A divergence between antisense plants and *rsw1-1* plants would not be unexpected because, if one can extrapolate from mRNA levels, antisense plants would have reduced amounts of catalytically normal glycosyltransferase, whereas *rsw1-1* would have normal levels of a modified enzyme. If such a specific mechanism is invoked to explain the lack of phenotype in antisense seedlings, it follows that antisense must more effectively produce the subcellular changes required to generate a phenotype in rosette leaves and inflorescences, situations where nothing is known about which subcellular changes cause phenotype development in *rsw1-1*. Although such explanations have some attractions, we cannot yet exclude that seedlings are inherently less susceptible to antisense suppression of any gene than are older plants.

Antisense Phenotype of *CesA2*

CesA2 expression was successfully reduced by the antisense construct but, compared with the *CesA1* and *CesA3* antisense phenotypes, we observed only a very mild morphological phenotype at 21°C. The phenotype is still subtle but becomes reproducible in plants grown at higher rates at 31°C. The reduced extension rate in the stem is consistent with a role in primary wall deposition, a role expected from the expression of a promoter-GFP construct in at least some dividing and expanding cells (J.E. Burn, unpublished data). This, therefore, brings the number of *CesA* genes implicated in primary wall deposition to four. Changes in secondary wall properties that might also be expected from the expression data showing expression in vascular tissue outside the elongation zone have not yet been found in the antisense plants and may be hard to document in practice if the changes are as small as those seen in elongation. The very mild height phenotype and the lack of detected effect on vessel element wall thickness in antisense plants may indicate that CesA2 makes only a small contribution to cellulose production or that the activity of another CesA enzyme renders it redundant. We should bear in mind, however, that it may be premature to assume that CesA2 glycosyltransferase activity has been successfully reduced because the relationship between reduced mRNA level and reduced protein level cannot be accurately predicted (Palomares et al., 1993).

Antisense Strategies for Functional Analysis of *CesA* Genes

Our work shows some of the advantages and limitations surrounding the use of antisense approaches to study *CesA* genes. Judged by the limited sampling of non-target *CesA* genes we undertook, the method can reduce expression of the target gene without affecting non-target genes. It also achieves a rather mild phenotype, which may be an advantage compared with null mutants where the severity of the defect may limit opportunities to assess gene function beyond the embryo. The two major limitations apparent from our work are (a) the instability of the phenotype, which makes it difficult to do analyses requiring large numbers of plants with uniform and predictable phenotypes, and (b) the very limited seedling phenotype that developed.

CONCLUSIONS

Antisense methods can specifically reduce the expression of *CesA* genes in Arabidopsis and establish the functions of at least some of them. *CesA3* expression was specifically reduced, and the morphological phenotype is consistent with *CesA3* depositing cellulose in primary walls. It shares this role with *CesA1* and *CesA6*, and all three give strong phenotypes

notwithstanding that *CesA3* and *CesA6* show redundancy for herbicide resistance. When stem growth is accelerated at 31°C, down-regulation of *CesA2* also slightly reduces stem elongation consistent with a role in primary wall synthesis for this gene as well. The reason why four CesA glycosyltransferases are required is still to be determined, but the case that CesA1 and CesA3 either serve different structural or enzymic functions or are differentially targeted within cells is further strengthened by the failure of a 35S::*CesA3* cDNA construct to complement *rsw1-1* when a 35S::*CesA1* cDNA construct does.

MATERIALS AND METHODS

Plant Growth

Plants of Arabidopsis were grown either in pots containing a 1:1:1 mix of peat:compost:sand, v/v) or aseptically on solid media in petri dishes. For routine growth of seedlings, seed was germinated on Murashige and Skoog (1962) medium containing 0.75% (w/v) agar and, when required, kanamycin (50 μg mL^{-1}). All plants were grown in growth cabinets at either 21°C or 31°C under continuous light (150 μmol m^{-2} s^{-1}).

Northern Analysis

Total RNA was extracted from 1 to 3 g of leaf, inflorescence, or root tissue using the appropriately scaled down method of Jacobsen-Lyon et al. (1995). Total RNA (25 μg) was run on 2.2 M formaldehyde/agarose gels and blotted onto positively charged nylon filters (Hybond N$^+$, Amersham, Buckinghamshire, UK). T7 polymerase transcription of linearized plasmids was used to generate antisense [^{32}P]UTP-labeled riboprobes. Filters were hybridized and washed as described by Dolferus et al. (1994) and exposed to phosphor screens (Molecular Dynamics, Sunnyvale, CA).

Gene-Specific Probes

PCR primers were designed to the first hypervariable region (Fig. 1) within the 5′ region of the *CesA1* genomic sequence (GenBank no. AF027172), the *CesA2* cDNA sequence (GenBank no. AF027173), the *CesA3* cDNA sequence (GenBank no. AF027174) and the *CesA10* genomic sequence (GenBank no. AC006300). *CesA1* forward, 5′-CGGGATCCCGAGTTCAATTACGCCCAGGGAG-3′; *CesA1* reverse, 5′-GGAATTCCGACGGGTCCACGATTCTTACAGGG-3′; *CesA3* forward, 5′-CGGGATCCCGTACTGTTGAGTTCAACTACC-3′; *CesA3* reverse, 5′-GGAATTCCGACATCTGATGAATAGGGAAGG-3′; *CesA2* forward, 5′-CGGGATCCCGAGTATGAGTTTGATCATGGG-3′; *CesA2* reverse, 5′-GGAATTCCTGAGGAACCATTGATCTCGC-3′; *CesA10* forward, 5′-CGGGATCCCGACATAGGTTTCTGGAGAGATTCCTA-3′; and *CesA10* reverse, 5′-GGAATTCCGAAGCAAAAGTTGATAGATACC-3′.

PCR products were cloned by digesting with *Bam*HI and *Eco*RI (restriction enzyme sites in primers underlined) and ligating into the vector pBluescript II SK− (Stratagene, La Jolla, CA). These clones were used to generate gene-specific probes for both northern and Southern analysis.

Construction of a Full-Length *CesA1* cDNA

A full-length cDNA of the *CesA1* gene was generated by annealing overlapping 5′ and 3′ fragments of the amplified gene from an Arabidopsis cDNA library (Arioli et al., 1998). The 5′ fragment was amplified with 5′-ACGCTCGAGTATTGAATCGGCTACG-3′ and 5′-AGACTATATTCCTGTTGG-3′. The 3′ fragment was amplified with 5′-ACTTTAATAACAGTAAGGC-3′ and 5′-GGCCTCGAGA-AACTTCAGATTCTTAGATAAA-3′ (*Xho*I sites underlined).

The two amplification products overlapped in a region that contained a unique *Bsp*HI restriction site. Digestion of both products with *Bsp*HI followed by a ligation, produced a full-length copy of the *CesA1* cDNA. The sequence of the full-length cDNA was confirmed before further cloning.

Generation of Antisense and Overexpression Constructs

An antisense *CesA1* construct was generated from the expressed sequence tag (EST) T20782 obtained from the Arabidopsis Stock Center (Columbus, OH). The EST clone was digested with *Xba*I and *Kpn*I and ligated into pGEM3Zf- (Promega, Madison, WI). The *CesA1* EST was removed from this recombinant plasmid by cutting with *Xba*I and *Sac*I and cloned into the binary vector pRD410 (Datla et al., 1992) replacing the *GUS* gene. This allows the *CesA1* fragment to be transcribed in the antisense orientation from the cauliflower mosaic virus 35S promoter. The *CesA1* sense construct was generated by cloning the full-length cDNA into the expression vector pART7 (Gleave, 1992) using the *Xho*I cloning sites. Constructs were identified that contained the *CesA1* gene in the sense orientation behind the cauliflower mosaic virus 35S promoter. The complete 35S::*CesA1* sense expression cassette was cloned into the *Not*I site of the binary vector pART27 (Gleave, 1992).

CesA3 antisense and sense constructs were made by digesting the full-length *CesA3* cDNA clone (Arioli et al., 1998) with *Not*I, filling the overhangs using Klenow polymerase, and ligating the entire cDNA into *Sma*I cut expression vector pART7. Antisense and sense clones were identified, and the entire expression cassette of each was removed with a *Not*I digest and ligated into the *Not*I site of the binary vector pART27.

A *CesA2* antisense construct was generated by digesting the *CesA2* cDNA with *Bam*HI. The 1.2-kb *Bam*HI fragment released from the 5′ end of *CesA2* was cloned into *Bam*HI cut pART7, and antisense constructs were identified. The entire expression cassette was removed from the recombinant pART7 by digestion with *Not*I and cloned into the *Not*I site of the binary vector pART27.

Production of Transgenic Plants

The recombinant binary constructs were introduced into *Agrobacterium tumefaciens* strain AGL1 by triparental mat-

ing. Eight pots of Arabidopsis ecotype Columbia containing approximately 16 plants per pot were vacuum infiltrated with AGL1 containing each construct (Bechtold et al., 1993). AGL1 carrying *CesA*1 and *CesA*3 sense constructs were infiltrated into *rsw1-1* (Arioli et al., 1998) grown at 21°C. Infiltration media contained 2.5% (w/v) Suc and 0.02% (v/v) Silwet L-77. Transformed plants were selected by germinating T_1 seed on Murashige and Skoog plates containing 50 μg mL^{-1} kanamycin and 100 μg mL^{-1} timentin.

Other Methods

Cryoscanning electron microscopy methods were described by Williamson et al. (2001). Cell wall thickness measurements were made on frozen stems snapped with a blade and freeze-etched before gold coating. Cellulose was determined by harvesting all rosette leaves from four 25-d-old T_3 plants of selected antisense lines and processing crude cell wall fractions as described by Lane et al. (2001) to determine cellulose as trifluoroacetic acid insoluble glucan. Measurements of stem growth rate and cell length were used to estimate cell flux, the rate at which cells exited the elongation zone in the growing stem (Silk et al., 1989). Bolt height was measured with a ruler at 2-d intervals for wild-type and *CesA3* antisense plants. All showed an approximately linear phase of growth, and the elongation rate (millimeters per day) was estimated from a graph for each plant. The lengths of 20 cells were measured by eyepiece micrometer on epidermal peels taken from stems of plants that had finished elongating. Peels were taken from sites containing cells that had emerged from the elongation zone during the linear phase of growth (d 10 for 21°C plants). Then elongation rate (millimeters per day) ÷ mean cell length (millimeters) = cell flux, the number of cells leaving the elongation zone in a 24-h period on d 10. To look at more rapidly growing plants, *CesA2* antisense plants and pBin19-transformed controls were grown at 31°C and measured in the same way. An exponential curve was fitted to the height data for each individual plant and an analysis of variance done using Genstat (version 5, release 4.2) to determine differences in the initial rate of elongation at the 5% significance level.

ACKNOWLEDGMENTS

We thank Roger Heady for assistance with cryoscanning electron microscopy and Josette Masle for timely assistance with statistical analysis.

Received October 11, 2001; returned for revision November 19, 2001; accepted February 1, 2002.

LITERATURE CITED

Arioli T, Peng L, Betzner AS, Burn J, Wittke W, Herth W, Camilleri C, Höfte H, Plazinski J, Birch R et al. (1998) Molecular analysis of cellulose biosynthesis in *Arabidopsis*. Science **279:** 717–720

Baskin TI, Betzner AS, Hoggart R, Cork A, Williamson RE (1992) Root morphology mutants in *Arabidopsis thaliana*. Aust J Plant Physiol **19:** 427–437

Bechtold N, Ellis J, Pelletier G (1993) In planta *Agrobacterium*-mediated gene transfer by infiltration of adult *Arabidopsis thaliana*. C R Acad Sci Ser III Sci Vie **316:** 1194–1199

Brown RM Jr, Saxena IM, Kudlicka K (1996) Cellulose biosynthesis in higher plants. Trends Plant Sci **1:** 149–156

Datla RSS, Hammerlindl JK, Panchuk B, Pelcher LE, Keller W (1992) Modified binary plant transformation vectors with the wild-type gene encoding NPTII. Gene **211:** 383–384

Dolferus R, Jacobs M, Peacock J, Dennis ES (1994) Differential interactions of promoter elements in stress response of the Arabidopsis Adh gene. Plant Physiol **105:** 1075–1087

Fagard M, Desnos T, Desprez T, Goubet F, Refregier G, Mouille G, McCann M, Rayon C, Vernhettes S, Höfte H (2000) *PROCUSTE1* encodes a cellulose synthase required for normal cell elongation specifically in roots and dark-grown hypocotyls of *Arabidopsis*. Plant Cell **12:** 2409–2424

Gleave AP (1992) A versatile binary vector system with a T-DNA organizational structure conducive to efficient integration of cloned DNA into the plant genome. Plant Mol Biol **20:** 1203–1207

Hauser MT, Morikami A, Benfey PM (1995) Conditional root expansion mutants of *Arabidopsis*. Development **121:** 1237–1252

Holland N, Holland D, Helentjaris T, Dhugga KS, Xoconostle-Cazares B, Delmer DP (2000) A comparative analysis of the plant cellulose synthase (CesA) gene family. Plant Physiol **123:** 1313–1324

Jacobsen-Lyon K, Jensen EO, Jorgensen JE, Marcker KA, Peacock WJ, Dennis ES (1995) Symbiotic and nonsymbiotic hemoglobin genes of *Casuarina glauca*. Plant Cell **7:** 213–223

Kimura S, Laosinchai W, Itoh T, Cui XJ, Linder CR, Brown RM Jr (1999a) Immunogold labeling of rosette terminal cellulose-synthesizing complexes in the vascular plant *Vigna angularis*. Plant Cell **11:** 2075–2085

Kimura S, Sakurai N, Itoh T (1999b) Different distribution of cellulose synthesizing complexes in brittle and non-brittle strains of barley. Plant Cell Physiol **40:** 335–338

Lane DR, Wiedemeier A, Peng L, Höfte H, Vernhettes S, Desprez T, Hocart CH, Birch RJ, Baskin TI, Burn JE et al. (2001) Temperature sensitive alleles of *RSW2* link the KORRIGAN endo-1,4-β-glucanase to cellulose synthesis and cytokinesis in *Arabidopsis thaliana*. Plant Physiol **126:** 278–288

Murashige T, Skoog F (1962) A revised medium for rapid growth and bioassays with tobacco tissue cultures. Physiol Plant **15:** 473–497

Nicol F, His I, Jauneau A, Vernhettes S, Canut H, Höfte H (1998) A plasma membrane-bound putative endo-1,4-β-D-glucanase is required for normal wall assembly and cell elongation in *Arabidopsis*. EMBO J **17:** 5563–5576

Palomares R, Herrmann RG, Oelmuller R (1993) Antisense RNA for components associated with the oxygen-

evolving complex and the Rieske iron/sulfur protein of the tobacco thylakoid membrane suppresses accumulation of mRNA, but not of protein. Planta **190:** 305–312

Pear JR, Kawagoe Y, Schreckengost WE, Delmer DP, Stalker DM (1996) Higher plants contain homologs of the bacterial *celA* genes encoding the catalytic subunit of cellulose synthase. Proc Natl Acad Sci USA **93:** 12637–12642

Peng L, Hocart CH, Redmond JW, Williamson RE (2000) Fractionation of carbohydrates in *Arabidopsis* seedling cell walls identifies three radial swelling loci that are involved specifically in cellulose production. Planta **211:** 406–414

Richmond T (2000) Higher plant cellulose synthases. Genome Biol **1:** 1–6

Ridge RW, Uozumi Y, Plazinski J, Hurley UA, Williamson RE (1999) Developmental transitions and dynamics of the cortical ER of *Arabidopsis* cells seen with green fluorescent protein. Plant Cell Physiol **40:** 1253–1261

Sato S, Kato T, Kakegawa K, Ishii T, Liu YG, Awano T, Takabe K, Nishiyama Y, Kuga S, Nakamura Y et al. (2001) Role of the putative membrane-bound endo-1,4-beta-glucanase KORRIGAN in cell elongation and cellulose synthesis in *Arabidopsis thaliana*. Plant Cell Physiol **42:** 251–263

Saxena IM, Brown RMJ, Fevre M, Geremia RA, Henrissat B (1995) Multidomain architecture of β-glycosyl transferases: implications for mechanism of action. J Bacteriol **177:** 1419–1424

Schatz PJ, Solomon F, Botstein D (1986) Genetically essential and nonessential alpha-tubulin genes specify functionally interchangeable proteins. Mol Cell Biol **6:** 3722–3733

Scheible W-R, Eshed R, Richmond T, Delmer D, Somerville C (2001) Modifications of cellulose synthase confer resistance to isoxalen and thiazolidinone herbicides in *Arabidopsis Ixrl* mutants. Proc Natl Acad Sci USA **98:** 10079–10084

Silk WK, Lord EM, Eckard KJ (1989) Growth patterns inferred from anatomical records: empirical tests using longisections of roots of *Zea mays* L. Plant Physiol **90:** 708–713

Sugimoto K, Williamson RE, Wasteneys GO (2001) Wall architecture in the cellulose deficient *rsw1* mutant of Arabidopsis: Microfibrils but not microtubules lose their transverse alignment before microfibrils become unrecognizable in the mitotic and elongation zones of roots. Protoplasma **215:** 172–183

Taylor NG, Laurie S, Turner SR (2000) Multiple cellulose synthesis catalytic subunits are required for cellulose synthesis in *Arabidopsis*. Plant Cell **12:** 2529–2539

Taylor NG, Scheible W-R, Cutler S, Somerville CR, Turner SR (1999) The *irregular xylem3* locus of *Arabidopsis* encodes a cellulose synthase required for secondary cell wall synthesis. Plant Cell **11:** 769–780

Turner SR, Somerville CR (1997) Collapsed xylem phenotype of *Arabidopsis* identifies mutants deficient in cellulose deposition in the secondary cell wall. Plant Cell **9:** 689–701

Williamson RE, Burn JE, Birch R, Baskin TI, Arioli T, Betzner AS, Cork A (2001) Morphology of *rsw1*, a cellulose-deficient mutant of *Arabidopsis thaliana*. Protoplasma **215:** 116–127

Zuo J, Niu QW, Nishizawa N, Wu Y, Kost B, Chua NH (2000) KORRIGAN, an *Arabidopsis* endo-1,4-β-glucanase, localizes to the cell plate by polarized targeting and is essential for cytokinesis. Plant Cell **12:** 1137–1152